Deep Water Pre-Processing: East Coast India

by

Phil Smith[1],
Ian F. Jones[1],
Dave King[1],
Pranaya Sangvai[2],
Ajoy Biswal[2],
&
Mohit Mathur[2]

1 ION GX Technology
2 Reliance Industries Ltd.

Corresponding author:
ian.jones@iongeo.com

Deep Water Pre-Processing: East Coast India

Phil Smith[1], Ian F. Jones[1], Dave King[1], Pranaya Sangvai[2], Ajoy Biswal[2], & Mohit Mathur[2]
1 ION GX Technology
2 Reliance Industries Ltd.

Corresponding author: ian.jones@iongeo.com

Introduction
The transition from shelf to deep water environments brings several specific challenges to the processing geophysicist. Out of plane scattered multiples hamper imaging of the deeper section, whilst near-sea-bed gas hydrate accumulations and channel-fill velocity anomalies cause distortions in images if these punctual velocity features are not correctly incorporated into the velocity model for depth migration (time imaging is an insufficient solution in these cases).

Building the velocity model of the subsurface with sufficient fidelity and resolution to overcome these issues, over large volumes of data, requires a combination of automated picking and detailed manual intervention for certain features. However, in order for an autopicker to work reliably, we first need to deliver clean pre-processed gathers, free of the effects of complex scattered 3D multiples. Consequently, best practise in imaging is inexorably linked to optimal pre-processing (the 'image-driven' concept).

In this paper, we describe our approach to tackling these problems, concentrating our attention on the pre-processing, specifically multiple suppression and scattered noise attenuation. We also touch on the iterative velocity model building and depth imaging for this project (described in Fruehn et al, 2008).

Multiple Suppression.
It is widely accepted that "direct" multiples are best attenuated using the surface related multiple elimination (SRME) technique (Verschuur, et al, 1992). Predictive deconvolution (Peacock & Trietel, 1969), parabolic Radon (Hampson 1986, Sacchi & Ulrych, 1995) and tau-p deconvolution (Yilmaz 1987) all fail to adequately attenuate direct water bottom multiples. However, tau-p deconvolution is often the most effective in attenuating the "peg-leg" multiples in shallow water. (Stewart, 2004; Stewart et al, 2007)

Traditionally, differential velocity based methods such as parabolic Radon have been used in deep water. These methods tend to fail on near offsets where locally there is little move-out difference between primaries and multiples. This problem becomes more serious with dip or where the multiple generators become more complex. Additionally, aliasing of the multiples on far offsets can lead to inadequate separation of primaries and multiples in transform space. This requires an additional de-alias step or a transform capable of handling aliased data. An alternative approach to interpolation for the de-aliasing is to perform the Radon transform in small overlapping windows within the CMP (the 'beam' Radon approach). Within each small sub-window in the CMP gather, the data 'appears' less aliased to the algorithm, as we are not attempting to decompose the complete (parabolic) trajectory in one step.

In recent years, the SRME technique has become popular in deep water. Near offset multiples in particular, are better attenuated with SRME than with parabolic Radon. Cascading 2D SRME and Radon became an industry standard approach. However, the complexity of the multiple generator and "out-of-plane" effects can severely limit this purely 2D combination. Radon-based techniques

fail for complex multiples, as the apex of the events in the CMP domain does not fall on zero offset for ray paths not in the plane of the shot-receiver axis. In these cases, an alternative method must be employed.

More recently, these cascaded 2D approximations have been superseded by 3D SRME, which is more correct from a theoretical viewpoint. 3D SRME models the true 3D ray-paths associated with free surface bounces from ocean-bottom and buried scatterers, as well as with complexities in the multiple wavefield resulting from the topography of the generating surface.

It can be shown that 2D SRME predicts multiple arrival times as being too great for out of plane scatterers. When the crossline dip exceeds about 10°, the 2D prediction will be too far removed from the actual arrival time for an adaptive subtraction to recover the error. In figure 1 (reproduced here from Stewart et al, 2007), we show the far-offset results of synthetic modelling of a shot with a single primary and its multiple, for an inline dip of 15° and crossline dip of 20°, and the corresponding position of the 2D SRME prediction of the multiple. The 3D SRME prediction gives correct arrival times for the multiple.

Despite the issues related to acquisition and sampling, 3D SRME has proved to be a powerful new tool in the arsenal of multiple attenuation techniques, and has been particularly successful for shelf-break irregularities off the east coast of India, in deep-water sub-salt applications in the Gulf of Mexico and Angola, and on corrugated sea-bed multiples in Norwegian waters.
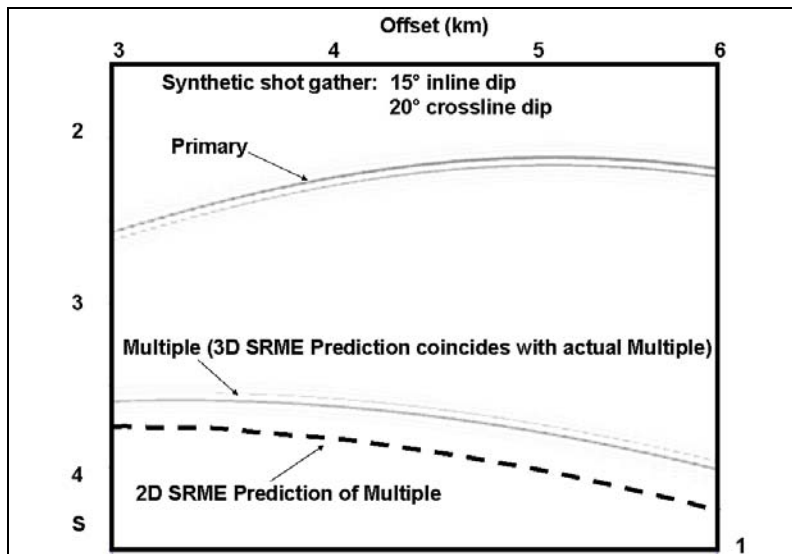

Figure 1. Synthetic shot gather from 3D ray-trace modelling through a model with both inline and crossline dip, showing primary and multiple, and the predicted position of the multiple from 2D SRME. The predicted position of the multiple from 3D SRME coincides with the actual multiple's position.

The Data
This project dealt with predominantly deep water (>1.5km) over an area of some 2100 sq.km. As part of the project, a 'fast-track' deliverable of a subset of the data was required (Sangvai, et al, 2008). Although the full area was processed through 3D SRME, in order to meet a tight turnaround deadline, the subset fast-track data (some 240 sq km input) was initially processed with 2D SRME (and later re-processed through full 3D SRME as part of the main project). Consequently, we have a good comparison of 2D versus 3D SRME through to 3D preSDM with all the associated pre-processing. These two volumes form the basis of the comparisons made here.

The data were initially put through de-spiking, swell noise attenuation and linear noise suppression routines. Thereafter, SRME was used followed by high resolution de-aliased (beams) parabolic Radon, apex-shifted multiple attenuation (ASMA), FX deconvolution, and high-cut filtering (100Hz in the shallow, 65Hz at depth). The latter steps were employed to attack non-surface-related classes of multiple, remnant noise, and aliased residual noise not modelled by the SRME. This aliased noise can be addressed using the 3D SRME approach directly, but it requires interpolation to a much denser trace spacing, and is not considered a cost effective approach, given that the remnant aliased noise can be very effectively removed using a beam-Radon technique.

Figure 2 shows a sample noisy shot record before and after suppression of swell noise and linear (cable tug) noise, and the difference QC plot. Removal of such acquisition noise, and spikes, renders the data suitable for passage through various 2D transforms. Without adequate de-noise processing, subsequent 2D transforms would spread the noise around the gather, irrevocably contaminating it.
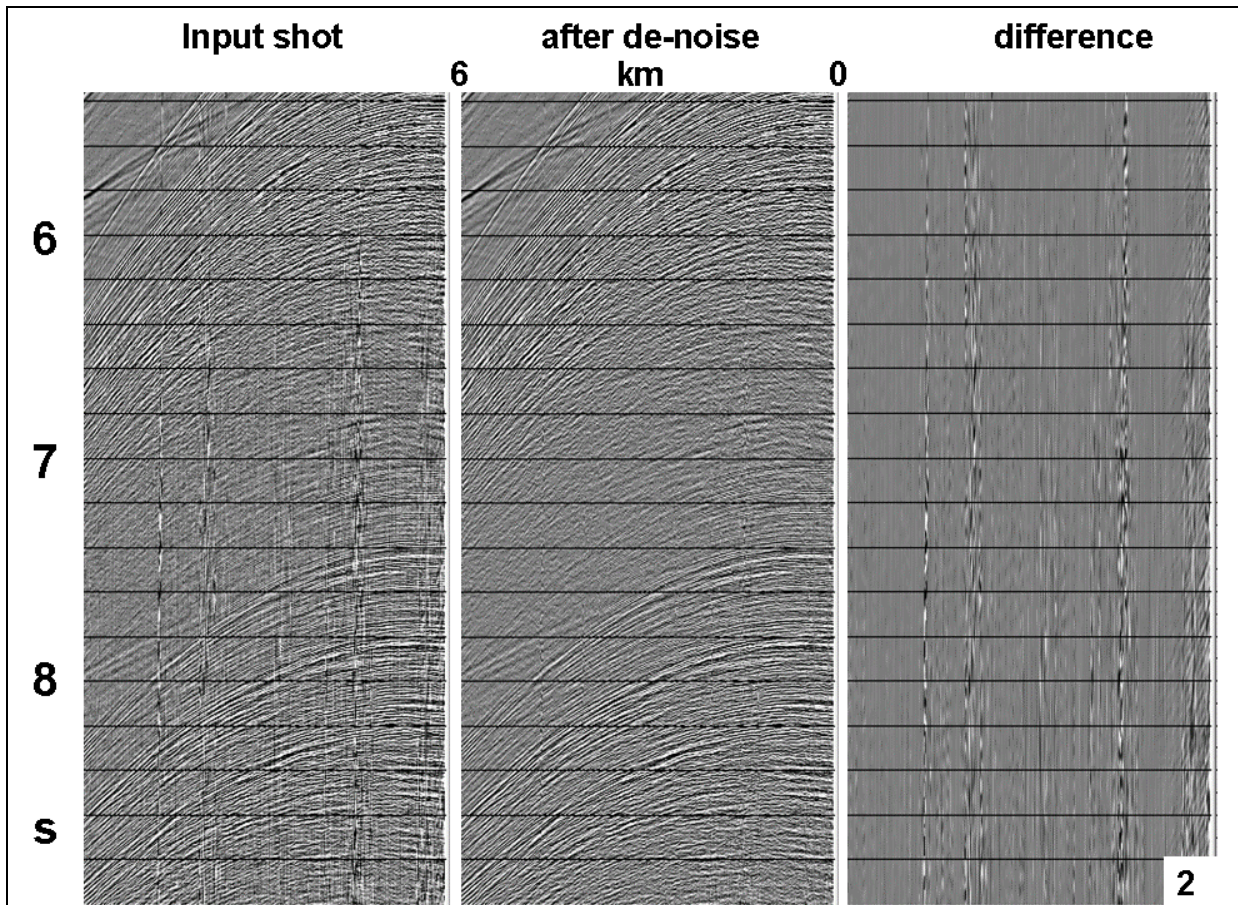

Figure 2. Sample noisy shot record before and after suppression of swell noise and linear (cable tug) noise, and the difference QC plot.

In figures 3 we show the progression of multiple suppression techniques used. Figure 3a shows the 2D SRME QC stack, indicating the location of the CMP gathers to be shown.; 3b shows the de-noise gathers (after NMO), whilst 3c – 3f show the gathers following cascaded application of 2D SRME, beam Radon, ASMA, and band pass filter. The end-product of these processing steps is ready for input to 3D preSDM and subsequent velocity autopicking.
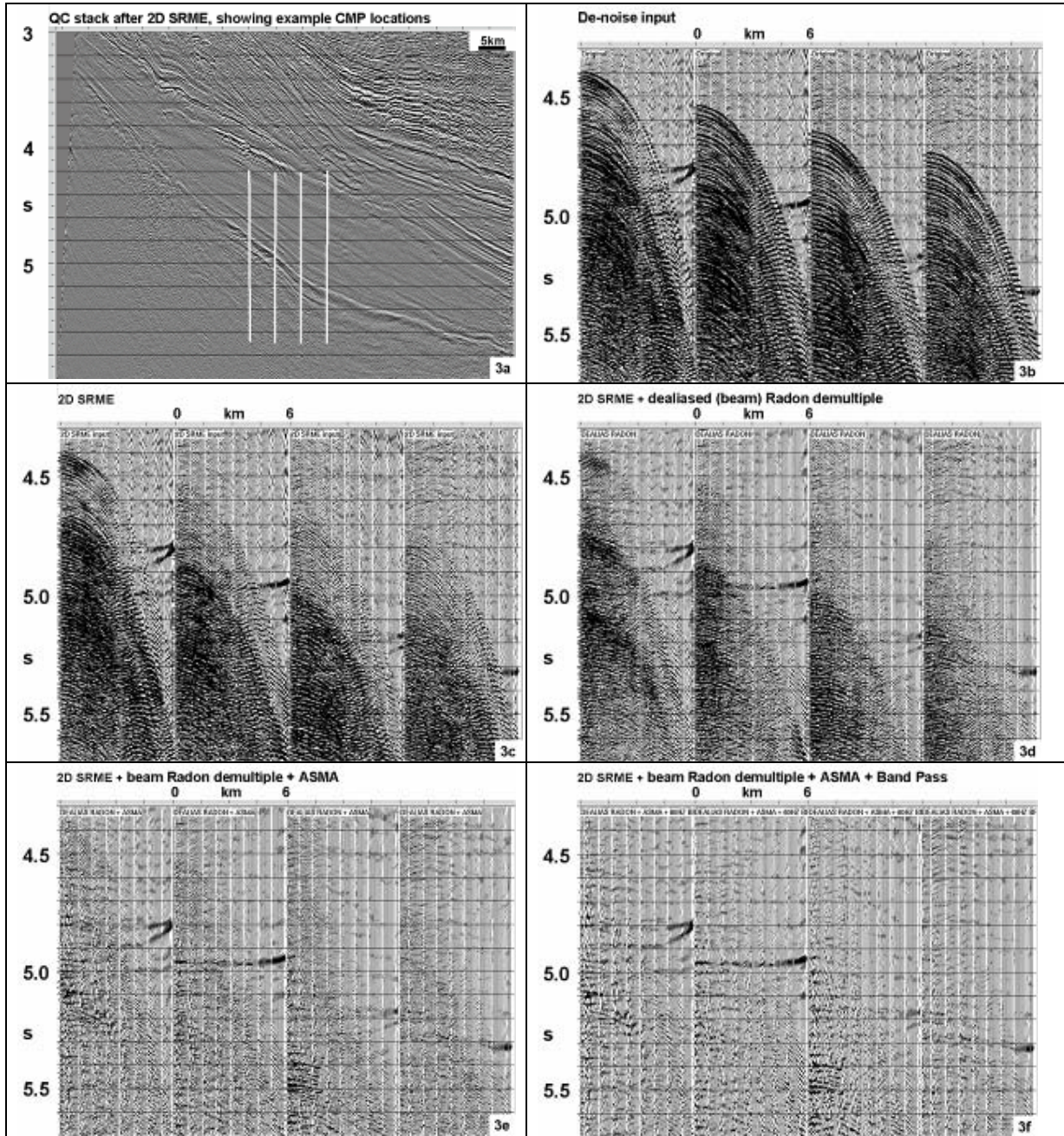
Figure 3. Progression of multiple suppression techniques used. 3a shows the 2D SRME QC stack, indicating the location of the CMP gathers; 3b shows the de-noise gathers (after NMO), 3c – 3f show the gathers following cascaded application of 2D SRME, beam Radon, ASMA, and band pass filter.

In figure 4, we show NMO'd data sorted to CMP gathers after application of the SRME technique (which is applied to shot gathers). We compare de-noised input data (4a) with results from 2D SRME (4b) and 3D SRME (4c). Complex ray-paths for the first sea-bed multiple and associated sedimentary layers, give-rise to a shifted-apex aspect to the moveout behaviour as seen in the CMP domain. Following either 2D or 3D SRME, additional de-noise techniques (as indicated in figure 3f) can be applied to deal with the aliased noise, other classes of noise, and non-surface related

multiple. We also show the result of applying this full post-processing sequence as well as an FX deconvolution, to the results for 2D SRME (4d) and for 3D SRME (4f).
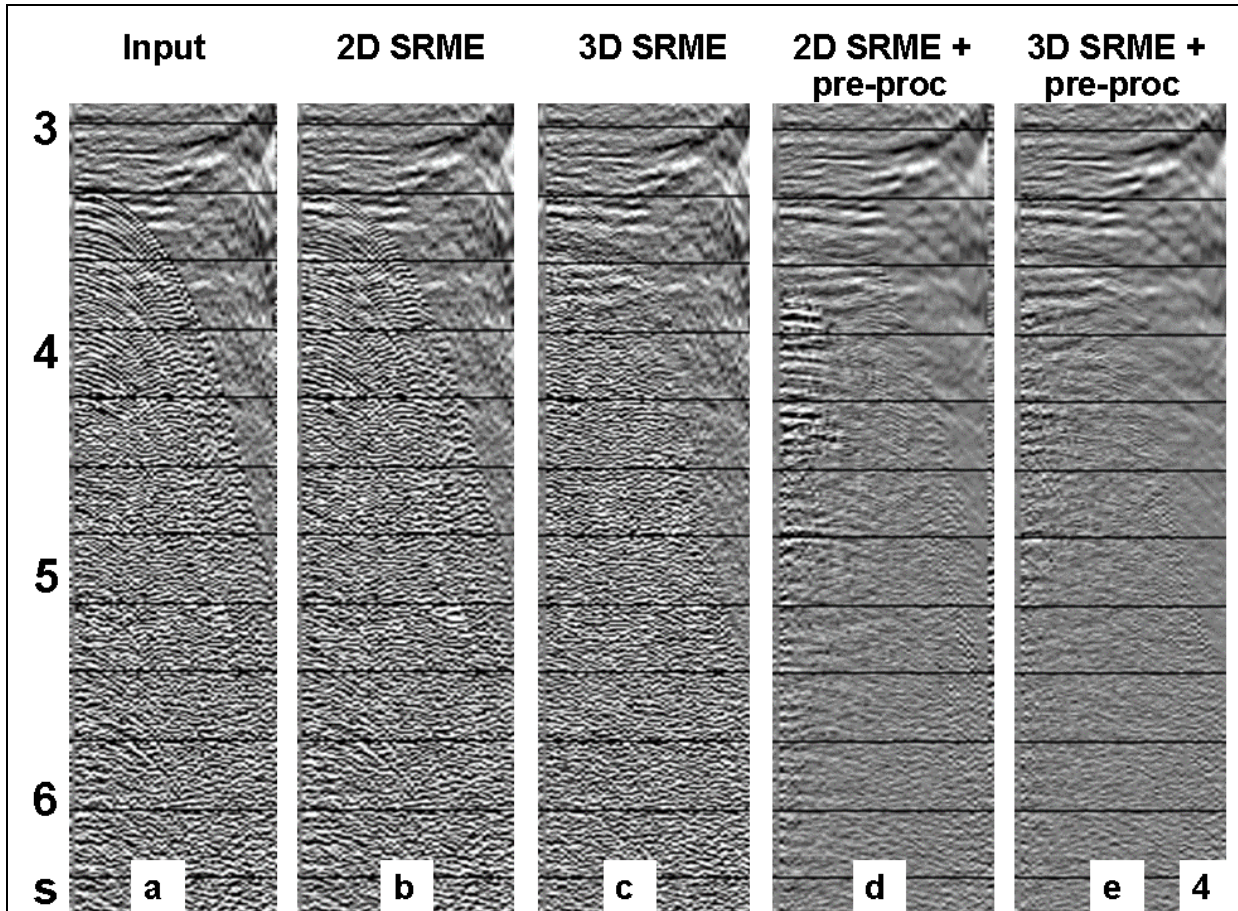

Figure 4. CMP gathers with 2nd order NMO. a) - input; b) - after application of 2D SRME; c) – after application of 3D SRME, d) 2D SRME + post processing; e) 3D SRME + post processing

In figure 5, we show the comparison as a QC crossline stack (prior to 3D preSDM). Figure 5a shows the 2D SRME, where we see a swath of noise sitting over an area of interest (a major unconformity near 4.4s). This remnant multiple energy will be spread around during migration and will be difficult to remove at that stage. Conversely, following 3D SRME (5b), the stack is mainly free of this multiple contamination. As part of the testing QC, a preSTM was performed on the 2D SRME and 3D SRME results, using the same velocity model. In figure 6a we see the preSTM of an inline for the 2D SRME data, whilst 6b shows the result after 3D SRME. Figure 6c shows the difference section, plotted with the same amplitude scaling as the other two sections. This gives a good indication of what has been missed by 2D SRME, and its effect via migration on the resultant image.
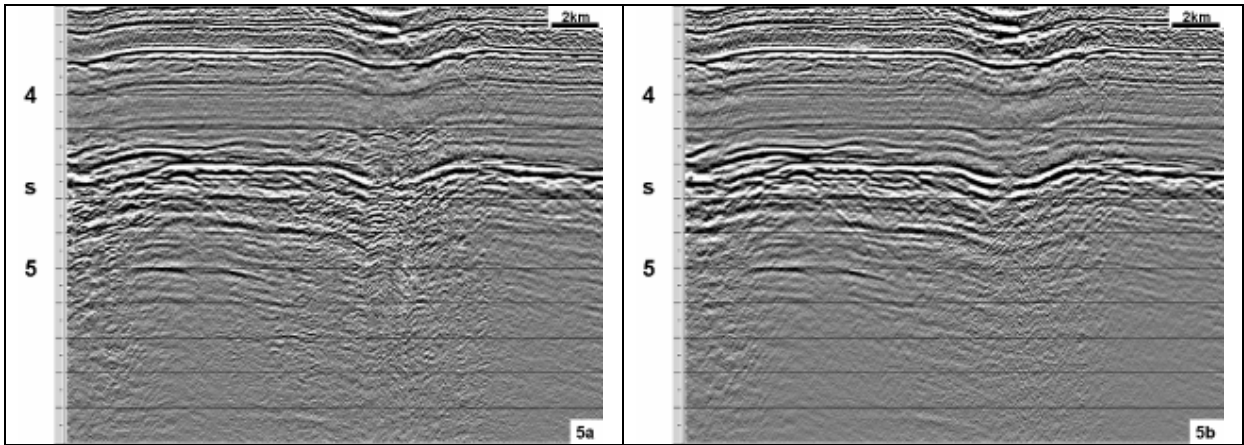
Figure 5. Unmigrated QC crossline stack, and QC preSTM. 5a shows 2D SRME result; 5b the 3D SRME result. A swath of noise sitting over a major unconformity near 4.4s is removed by the 3D SRME. The remnant multiple energy from the 2D SRME result will be spread around during migration and will be difficult to remove at that stage.
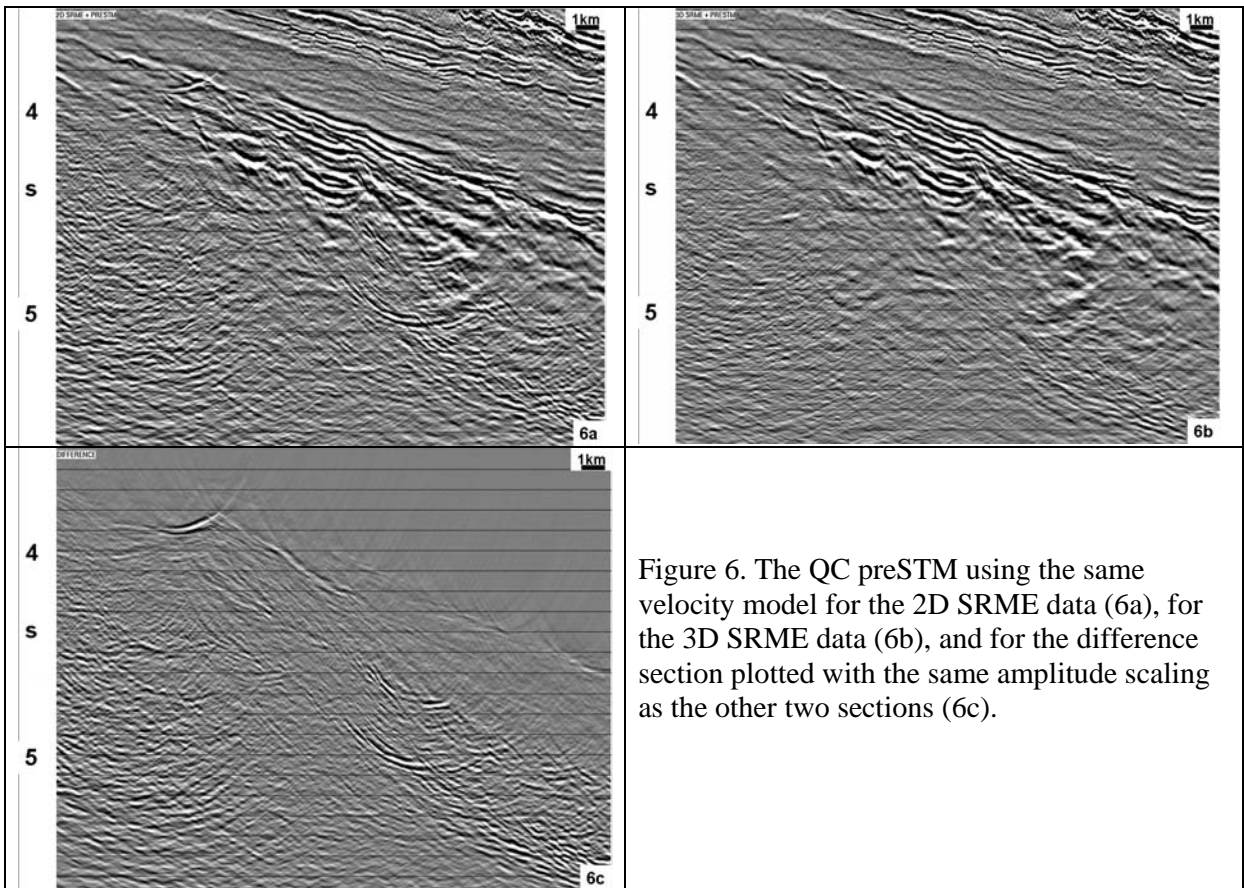

Figure 6. The QC preSTM using the same velocity model for the 2D SRME data (6a), for the 3D SRME data (6b), and for the difference section plotted with the same amplitude scaling as the other two sections (6c).

Velocity Model Building & Pre-Stack Depth Migration
In an environment with punctual discontinuous velocity anomalies, such as those associated with narrow channel fills or gas hydrate accumulations, a purely layer based velocity model will be inadequate (Jones, 2003). Furthermore, a purely gridded approach may also encounter problems (Jones, et al, 2007).

Deep Water Pre-Processing: Smith, et al, 2008

In this project, we used a hybrid-gridded approach, where we combined conventional gridded tomography, high resolution gridded tomography, auto-picked layers, and detailed manually interpreted layers (Fruehn et al, 2007, 2008). The initial depth interval velocity was derived from the time-stacking velocity (smoothed and converted to depth interval velocity), and the water bottom was picked from a water-velocity depth migration and inserted in the initial model as an explicit layer. The water velocity was selected from a migration-perturbation scan.

Following this, several iterations of gridded tomographic model update were performed. This involves running an autopicker (in this instance based on plane-wave destructors - Claerbout, 1992; Hardy, 2003) on densely sampled CRP depth gathers, and inputting the autopicked velocity errors and dip information to the gridded tomographic 3D solver. The solver is a conjugate gradient technique, able to handle large 3D volumes.

For possible free-gas accumulations beneath gas hydrate layers, we relied primarily on high resolution gridded tomography, and were able to resolve small-scale velocity features with interval velocity ~ 1250m/s, compared with the background sediment velocities of ~1600m/s. For detailed narrow channels, we relied on manual interpretation of the top and base of the channel features, and a scan over potential channel-fill velocities.

In figure 7, we extend the comparisons of 2D versus 3D SRME and show the results after 3D preSDM. The migration following application of 2D SRME (7a) over the priority 'fast-track' area shows a swath of noise sitting over an area of interest (a major unconformity). This remnant multiple energy has been spread around during migration and is difficult to remove at this stage. Conversely, following 3D SRME on the full volume (7b), the migration is mainly free of this multiple contamination. (Note that the 3D SRME data also had trace regularization prior to migration, but this is of secondary importance, and that the velocity model had further refinement after application of 3D SRME, so this comparison is not absolutely valid, but is sufficient to give a good indication of the effect of 3D SRME).
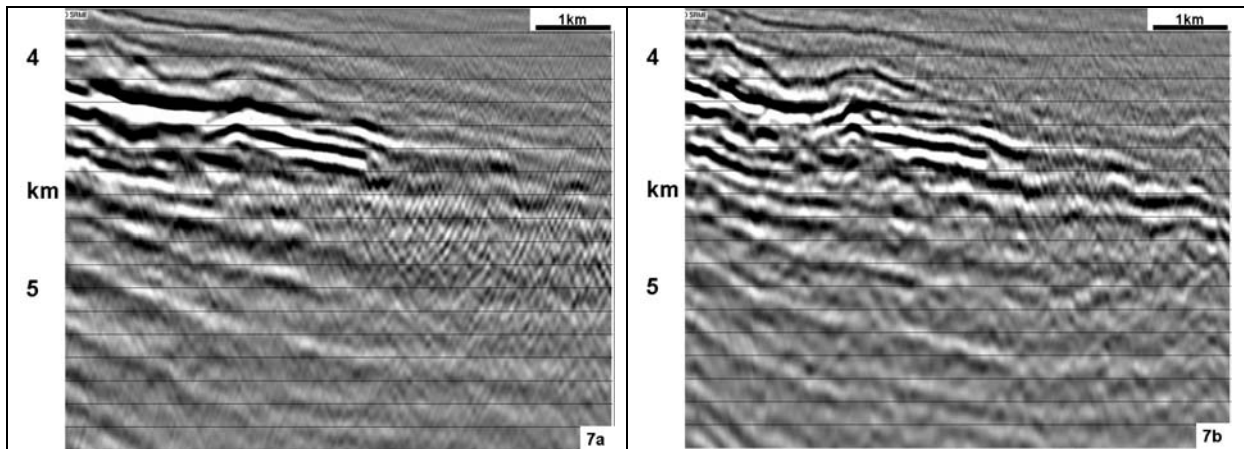

Figure 7. 3D preSDM following application of 2D SRME (7a) and 3D preSDM following application of 3D SRME and trace regularization (7b). Note that these images have different velocity models below about 5km, as the deep section's model was updated following 3D SRME, but these differences are insignificant compared to the noise reduction.

These results constitute an improvement over the existing 2004 3D preSTM (which had 2D SRME), both for the shallow section, where pull-down effects have been removed for the most-part, and in the deeper section were previously the scattered remnant multiples obscured potential targets. In figure 8, we compare an inline from the preSTM (8a) with the preSDM results (8b). The final preSDM was output to 15km depth, but in this display, 12km have been converted to time for

comparison. The preSDM image shows an increased clarity in the vicinity of the unconformity thanks to removal of remnant multiple energy by 3D SRME. In the preSTM we have lateral mispositioning shifts of about 1.5km at a two-way time of 6s (~9km depth) on the steeper events on the left of the section, due to time migration's inherent mis-treatment of ray-bending.

In figure 9, we make a similar comparison on an inline of the vintage preSTM (9a) with the results in depth for the preSDM (9b). The improvement in multiple suppression in the 3D SRME result is significant.

For the data under consideration, we do not face any classical multi-pathing problems (a ray-trace modelling study indicated that the velocity ratio between the low velocity anomalies and the surrounding sediments was not sufficiently large as to produce multi-pathing), hence for the final migration, an amplitude preserving Kirchhoff implementation is well suited for the problem, and was used here.

Conclusions

For imaging in complex environments, it is necessary to employ a wide range of tools for suppression of the various classes of noise and multiple. This must be accomplished in the pre-stack domain so that automated dense picking can be performed on migrated gathers to permit reliable model update. A diverse toolkit for noise and multiple attenuation, combined with a flexible model building system, and amplitude preserving imaging algorithms are necessary prerequisites to successfully accomplish this task.

Utilization of such an approach for data offshore eastern India has resulted in an improvement in image quality compared to a recent pre-stack time migration, avoiding the structural distortion introduced by localized velocity variation in the near surface sediments, delivering gathers suitable for attribute work.

The integration of client interpretational expertise in the model building stages of the process is invaluable. Such integration allows the interpreter to gain ongoing insight into the behaviour of the geology during the progress of the model building, such that additional effort can be targeted at areas of interest as required.
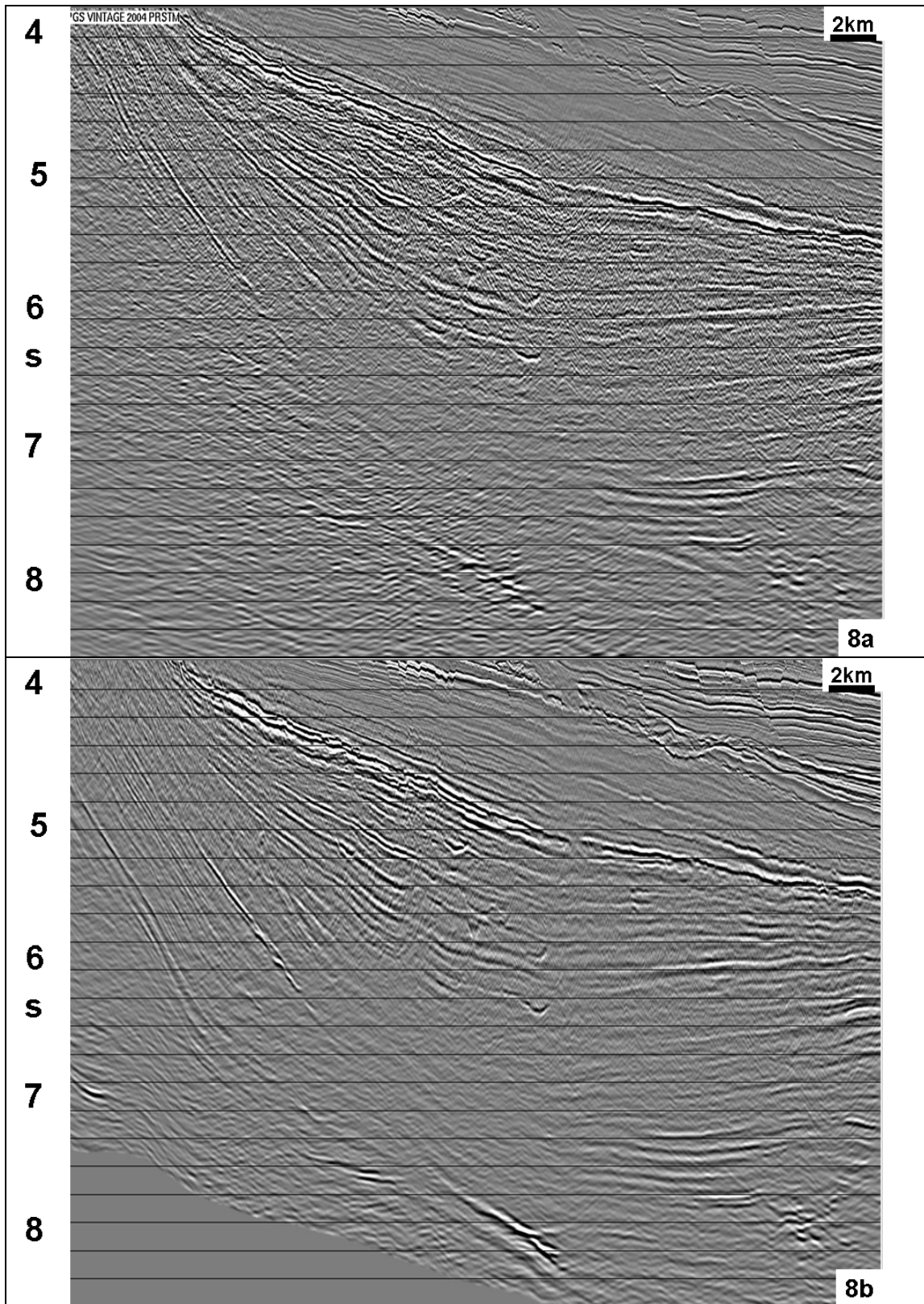
Acknowledgements

Figure 8. Inline results from the vintage 2004 3D preSTM (8a) which had 2D SRME and the (time converted) new 2007 3D preSDM (8b). The preSDM image shows an increased clarity in the vicinity of the unconformity thanks to removal of remnant multiple energy by 3D SRME. In the preSTM we have lateral mispositioning shifts of about 1.5km at a two-way time of 6s on the steeper events.
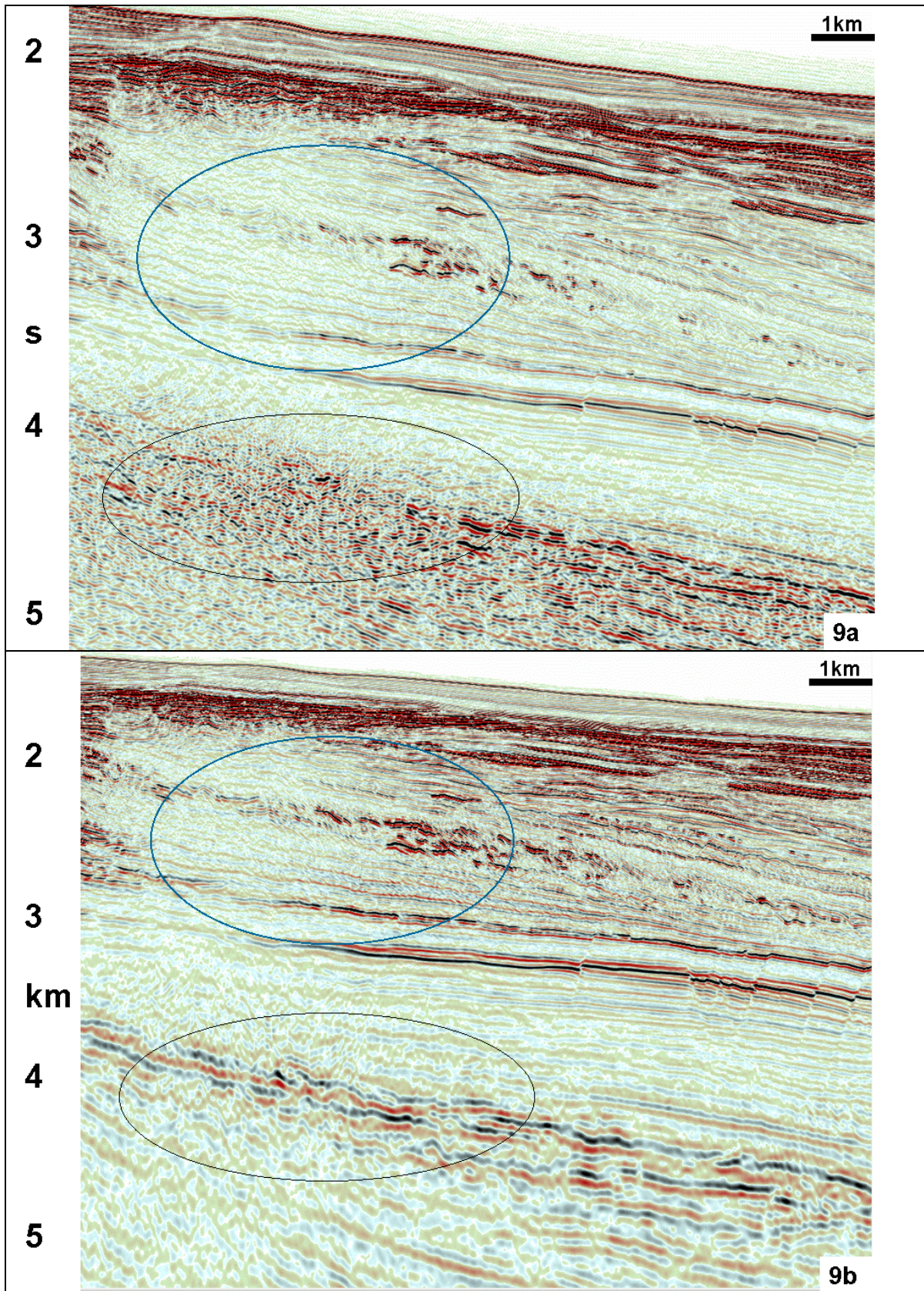
Figure 9. Inline comparison of the vintage 2004 3D preSTM (9a) with the results in depth for the new 2007 3D preSDM (9b). The improvement in multiple suppression in the 3D SRME result is significant.

Deep Water Pre-Processing: Smith, et al, 2008

References

Claerbout, J.F., 1992, Earth Soundings Analysis: PVI, Blackwell Scientific Publications.

Fruehn, J., Sherazi-Selby, H., Hardy, P., Tytri, J., and Steinsland N., 2007, High-resolution velocity model-building for pre-stack depth migration in the Nordsjøn area, Norwegian North Sea: EAGE proceedings.

Fruehn, J.K., Jones, I. F., Valler, V., Sangvai, P., Biswal, A., & Mathur, M., 2008, Resolving Near-Seabed Velocity Anomalies: Deep Water Offshore South East India: Geophysics, in press.

Hampson, D., 1986, Inverse velocity stacking for multiple ellimination. J. Can. Soc. Expl. Geophysics, 22, 1, 44-55

Hardy, P.B., 2003, High resolution tomographic MVA with automation: SEG/EAGE summer research workshop, Trieste.

Jones, I.F., 2003, A review of 3D preSDM velocity model building techniques: First Break, 21, No.3, 45-58.

Jones, I.F., Sugrue, M.J., Hardy, P.B., 2007, Hybrid Gridded Tomography: First Break, v25, No.4, 15-21.

Peacock, K.L., Treitel, S., 1969: Predictive Deconvolution: Theory and Practice: Geophysics, 34, 155-169.

Sacchi, M.D., Ulrych, T.J., 1995, High-Resolution velocity gathers and offset space reconstruction: Geophysics, 60, 1169-1177.

Sangvai, P., Biswal, A., Mathur, M., Fruehn, J.K., Smith, P., King, D.G., Jones, I. F., and Goodwin, M.C., 2008: Complex Imaging Challenges: Offshore South East India: Proceedings of the 7th biennial meeting of the SPG, Hyderabad.

Stewart, P., 2004, Multiple attenuation techniques suitable for varying water depths: Proceedings of the CSEG annual meeting.

Stewart, P.G., Jones, I.F., Hardy, P.B., 2007, Solutions for deep water imaging: Geohorizons, January, 8-22.

Verschuur, D.J., Berkhout, A.J., Wapenaar, C.P.A, 1992: Adaptive Surface Related Multiple Elimination: Geophysics, 57, 1166-1177.

Yilmaz, O., 1987: Seismic Data Processing: Society of Exploration Geophysicists.